



## Isolation of Cinnamaldehyde and its application as a green corrosion inhibitor for A03081 alloy in 2.0 M HCl solution: Theoretical, Electrochemical and Thermodynamics studies

Asmaa A. I. Ali, El-Sayed M. Mabrouk, Noura Gamal, Ali Y. El-Etre,  
Doaa F. Seyam \*



<sup>1</sup>Chemistry Department, Faculty of Science, Benha University, Benha, Egypt

### Abstract

Isolation of Cinnamaldehyde from Cinnamon was executed successfully. The structure of Cinnamaldehyde was confirmed using FTIR, <sup>1</sup>H NMR, <sup>13</sup>C NMR and mass spectroscopies. Chemical, electrochemical and thermodynamic measurements were employed to study Cinnamaldehyde behavior as a corrosion inhibitor for aluminum in acids. The results showed that Cinnamaldehyde molecules tend to adsorb on the aluminum surface covering it from the attacking acidic medium, with %IE = 93.24% after 24 h. Temkin adsorption isotherm is fitted with the results excellently, that the adsorption process was considered spontaneous and predominantly physical, with  $\Delta G^{\circ}_{ads}$  values reached -35 kJ.mol<sup>-1</sup>. Thermodynamic parameters were estimated and discussed. SEM analysis and quantum study were conducted to support the inhibition capability of the extract.

Keywords: Corrosion, inhibition, aluminum, quantum, Monte Carlo, plant extract.

### 1. Introduction

Corrosion is formed from the oxidation of the surface atoms of metals when contacted with moistured atmospheric oxygen [1]. Since it has so many uses, like oil and gas recovery tasks, extraction, and acid descaling, research on aluminum corrosion in acidic conditions is becoming increasingly popular in the scientific as well as industrial communities [2]. Because aluminum alloys are cheap, easy to handle, and have good conductivity for both electricity and heat, they are used in a wide range of industries, including manufacturing, electrical engineering, containers and means of transportation. With a yearly market of 25 million tons, aluminum is the most popular nonferrous metal in metallurgical technology. The growth of an oxide layer that firmly holds aluminum's surface is the most significant characteristic of its corrosion vulnerability. Deterioration of the aluminum oxide layer can be limited by careful machine maintenance and washing, but it is very difficult to reduce chemical deterioration caused by environmental factors; at pH values below 4.0 and above 9.0, the oxide layer becomes soluble.

The expression "green inhibitor" or "eco-friendly inhibitor" refers to compounds that are nontoxic naturally and have the efficiency to inhibit metal corrosion. Therefore, a lot of researches have been conducted and green inhibitors were recommended. Al-Turkustani et al. [3] examined how well Aloe extract works as a natural inhibitor to stop aluminum from corroding in 0.5M HCl [3] and also, examined how well the Ajowan plant's aqueous extract prevented aluminum corrosion in an acidic solution [4]. Singh et al [4] extracted berberine, a yellow isoquinoline alkaloid dye, from the root extract of *Coptis chinensis*. Berberine's ability to prevent aluminum alloy corrosion in a 3.5% NaCl solution was investigated. Mayakrishnan, et al [5] examined the anticorrosion properties of the plant extract from *P. odoratum*, a green inhibitor for aluminum. El-Katori and S Al-Mhyawi [6] investigated a cheap and eco-friendly inhibitor for aluminum in 1.0 M H<sub>2</sub>SO<sub>4</sub> via the *Bassia muricata* extract. Thi Huong Pham et al [7] increased the Al-air battery's capacity by using chrysanthemum coronarium leaves extract (CCLE) to inhibit the corrosion of Al anodes. Kwolek et al [8] examined gallic acid, which is present in a variety of foods and plants, including tea, as a green corrosion inhibitor for aluminum in an aqueous solution of orthophosphoric acid. Chowdhury et al 2023 looked into how well tulsi and green tea extracts inhibited corrosion in an acidic environment for aluminum and its alloys [9]. Méndez et al [10] investigated the extract of *Ilex paraguariensis* (Yerba Mate) as a potential environmentally friendly anti-corrosion agent for aluminum in HCl solution. Chamomile flower extract (CFE) is employed by Abdullah [11] as an ecologically safe and sustainable material to protect aluminum in saltwater.

\*Corresponding author e-mail: doaa.fouad17@fsc.bu.edu.eg.; (Doaa F. Seyam).

Received date 02 March 2025; Revised date 18 March 2025; Accepted date 13 April 2025

DOI: 10.21608/ejchem.2025.364505.11376

©2025 National Information and Documentation Centre (NIDOC)

To the best of our knowledge, Cinnamaldehyde was not used previously to prevent aluminum from corroding in acidic environments. For being eco-friendly plant extract, Cinnamaldehyde is considered acceptable as a potential green corrosion inhibitor in industry. Since Cinnamaldehyde has active sites that accelerate the adsorption process, high inhibition efficiency is expected. The aim of this work deals with Cinnamaldehyde isolation from Cinnamon. Its structure was confirmed and then was tested as a green inhibitor against corrosion of A03081 alloy in 2.0 M HCl solution.

## 2. Experimental

### 2.1. Materials

The composition of A03081 alloy used in this investigation, in (w/w %) is: Si (6.0), Cu (4.0), Mg (0.1), Zn (1.0), Fe (0.8), V (0.05), Mn (0.5), Ti (0.25), and Al (remainder). The alloy is given by the Egyptian Copper Works Company, Egypt. Acetone, ethanol (99%), chloroform and HCl were gotten from AL-Nasr Chemicals Co., Egypt.

### 2.2. Cinnamaldehyde extraction

A quarter of a kilo of cinnamon was ground, put in a cotton bag, and put in a Soxhlet for two days. The solution was then evaporated till it became oily. The solvent used was chloroform, **Figure 1**.

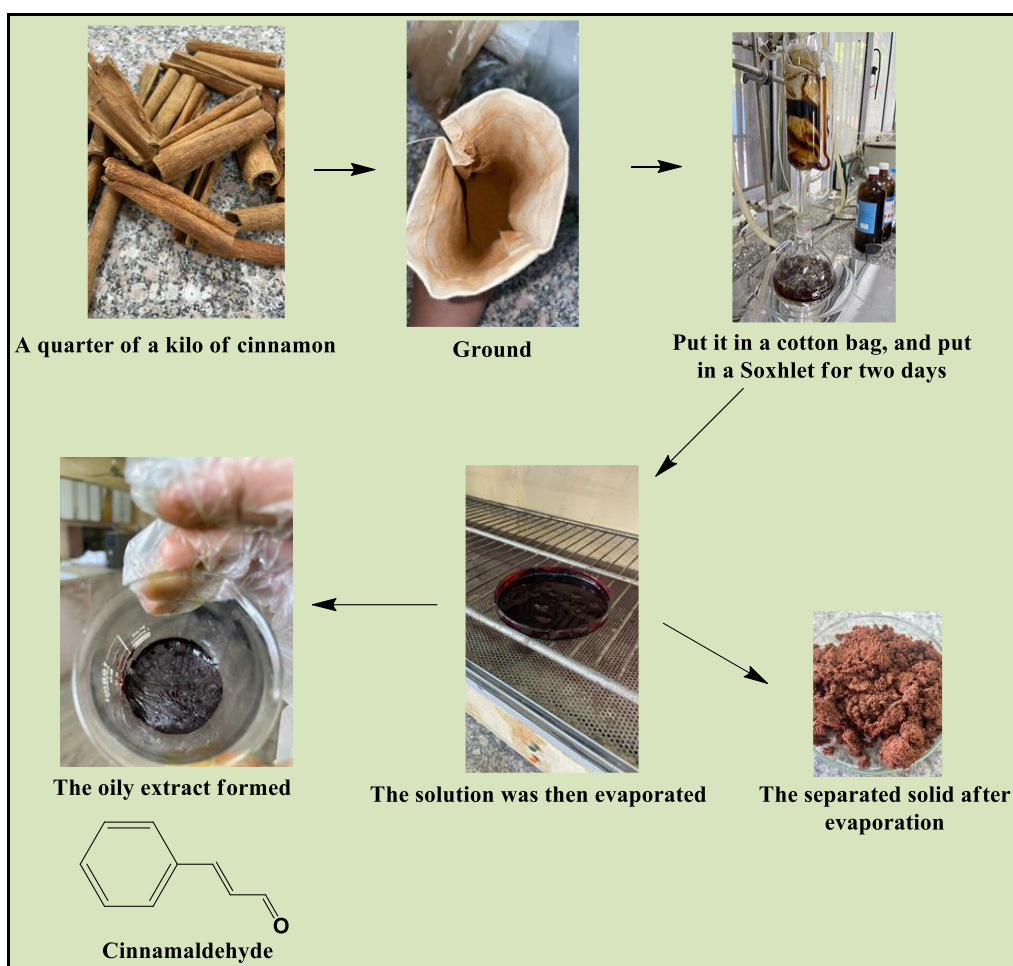


**Figure 1:** Cinnamaldehyde extraction

### 2.3. Structure elucidation

The infrared spectrum was run on Thermo Scientific Nicolet iS10 FTIR spectrometer using KBr as a carrier. The  $^1\text{H}$  NMR and  $^{13}\text{C}$  NMR spectra were also measured using Varian Mercury-300 NMR Spectrometer. The  $^1\text{H}$  NMR was performed with resonance frequency of 300 MHz at 303 K, and the solvent used is  $\text{CD}_3\text{OD}$ . The  $^{13}\text{C}$  NMR was performed with resonance frequency of 75 MHz at 303 K, and the solvent used is  $\text{CDCl}_3$ . Molecule

fragments were identified by Thermo Scientific, USA, Trace GC Ultra/ISQ Single Quadrupole MS, TG-5MS detection, with ionization energy of 70 eV.

**FTIR (KBr)  $\text{cm}^{-1}$   $\nu_{\text{max}}$ :** FTIR spectrum showed characteristic bands at 3027, 3057, 3110  $\text{cm}^{-1}$  ( $\nu_{\text{CH}}$  Ar), 1590  $\text{cm}^{-1}$  ( $\nu_{\text{C=O}}$ ), 1467  $\text{cm}^{-1}$  ( $\nu_{\text{C=C}}$  Ar), **Figure S1**.

**$^1\text{H}$  NMR (300 MHz,  $\text{CD}_3\text{OD}$ )  $\delta$ :**  $\delta$  9.71 – 9.66 (dd,  $J = 7.1, 1.3$  Hz, 1H, 10), 7.58 – 7.53 (m, 2H, 4, 6), 7.53 – 7.46 (m, 1H, 12), 7.44 – 7.37 (m, 2H, 1, 3), 7.37 – 7.30 (m, 1H, 2), 6.70 – 6.62 (m, 1H, 13), **Figure S2**.

**$^{13}\text{C}$  NMR (75 MHz,  $\text{CDCl}_3$ )  $\delta$ :** 181.79, 155.89, 138.73, 129.65, 127.14, 124.94, 122.51, **Figure S3**.

**Mass Spectrum (EI-MA):**  $m/z$  ( $\text{C}_9\text{H}_8\text{O}$ ) = 132.93 [ $\text{M}^+$ ], with relative abundance (18.77%), **Figure S4**.

## 2.4. Stock preparation

1000 mg of the extract is dissolved in a least amount of ethanol (99%), then continued with distilled water till 1 liter, and the appropriate concentrations (10, 40, 80, 120 and 200 ppm) were prepared by dilution with distilled water.

## 2.5. Weight loss (WL) measurements

The weight loss measurements were done using A03081 alloy coupons of  $3 \times 1.5 \times 1 \text{ cm}^3$  dimensions in 2.0 M HCl solution with different concentrations of Cinnamaldehyde extract; 0, 10, 40, 80, 120 and 200 ppm. The coming equations were utilized to calculate both the inhibition efficiency and the surface coverage [12, 13]:

$$\%IE_{WL} = \left(1 - \frac{CRt_{WL,Cin}}{CRt_{WL}}\right) \times 10 \quad (1)$$

$$\theta = \left(1 - \frac{CRt_{WL,Cin}}{CRt_{WL}}\right) \quad (2)$$

where,  $CRt_{WL,Cin}$  and  $CRt_{WL}$  ( $\text{mg}\cdot\text{h}^{-1}\cdot\text{cm}^{-2}$ ) are the corrosion rate of A03081 alloy in inhibited (using Cinnamaldehyde extract) and uninhibited 2.0 M HCl solution.

## 2.6. Electrochemical measurements

Potentiodynamic polarization (PDP) and electrochemical impedance spectroscopy (EIS) of A03081 alloy in 2.0 M HCl solution without and with 10, 40, 80, 120 and 200 ppm Cinnamaldehyde extract were conducted using SP-150 Potentiostat with EC-Lab software. The electrochemical cell used in the current study was a three-electrode system cell (the working electrode; the A03081 alloy, the reference electrode; an SCE and the counter electrode; a platinum electrode). The scan rate used in PDP was 1 mV/s and the frequency range for EIS was from 100 KHz to 0.1 Hz.

## 2.7. SEM analysis

The surface morphology of A03081 specimens was examined using a JSM-IT700HR/LA SEM. This device was used for scanning electron imaging using a 15 kV accelerating voltage when A03081 coupon was merely surface polished and submerged for 3 h in 2.0 M HCl without as well as with 200 ppm of the extract present. This instrument produced a 500X magnification.

## 2.8. Quantum and Monte Carlo simulations

Optimization of Cinnamaldehyde structure was done using Gaussian 09 program by applying B3LYP/3-21G method. Monte Carlo simulations of Cinnamaldehyde adsorption on aluminum was performed using Materials Studio 2020 program by adsorption simulation of one Cinnamaldehyde molecule and 50 molecules of both  $\text{H}_2\text{O}$  and HCl, to simulate the aggressive medium on Al (001) surface with space group (194) P63/mmc, in a ( $48.309 \times 48.309 \times 71.635 \text{ \AA}$ ) boundary box, with a 101.671  $\text{\AA}$  slab-thickness, and a ( $5 \times 5$ ) supercell.

## 3. Results and Discussion

### 3.1. Weight loss (WL) measurements

According to **Figure 2** and the data in **Table 1**, corrosion rate clearly decreased as Cinnamaldehyde content increased, with a tendency to a plateau after 10 hours. This shows that the extract particles moved toward the A03081 alloy surface in the early hours and adhered to it, creating a barrier between the A03081 alloy surface and the acidic medium, reducing the alloy's corrosion [14]. Till less than 200 ppm, since there were more protective molecules on the A03081 alloy surface with higher concentrations, the Cinnamaldehyde's effectiveness rose

as concentration did as well. Additionally, the steadiness of the efficiency after 10 h demonstrates how the adsorption process depleted the extract in the solution during the first hours of exposure. The Cinnamaldehyde structure revealed heteroatoms like O, the benzene ring, and  $\pi$  electrons that are in charge of the attraction between the inhibitor molecules and the A03081 alloy surface, followed by the adsorption, hence inhibition action [15].

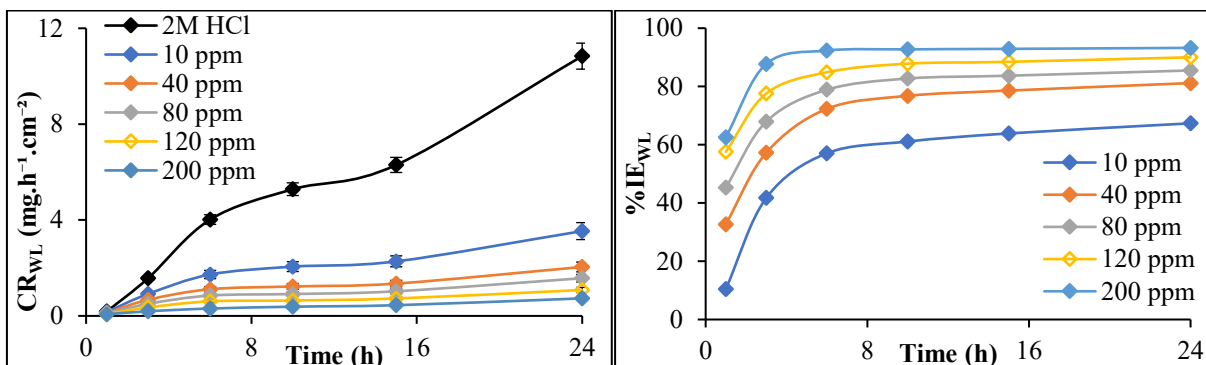


**Figure 2:** The corrosion rate of A03081 alloy and inhibition efficiency of different Cinnamaldehyde concentrations vs. time in 2.0 M HCl (relative standard uncertainty [ur] limit is  $\pm 5\%$ )

**Table 1:** The corrosion rate ( $CR_{TWL}$ ) in  $mg.h^{-1}.cm^{-2}$  of A03081 alloy and inhibition efficiency of varying Cinnamaldehyde concentrations in 2.0 M HCl solution, at 298 K for different exposure hours

Time (h)	Blank		10 ppm		40 ppm		80 ppm		120 ppm		200 ppm	
	$CR_{TWL}$	%IE <sub>WL</sub>										
1	0.18	0.16	10.49	0.12	32.70	0.10	45.31	0.08	57.56	0.07	62.57	
3	1.57	0.92	41.73	0.67	57.23	0.50	67.92	0.35	77.56	0.19	87.73	
6	4.02	1.73	57.06	1.11	72.32	0.85	78.88	0.61	84.88	0.31	92.35	
10	5.29	2.06	61.10	1.23	76.77	0.91	82.72	0.64	87.82	0.38	92.74	
15	6.30	2.28	63.87	1.35	78.58	1.03	83.69	0.73	88.46	0.45	92.91	
24	10.84	3.54	67.35	2.04	81.16	1.57	85.49	1.08	90.02	0.73	93.24	

## 3.2. Electrochemical Measurements

### 3.2.1. Potentiodynamic Polarization Measurements (PDP)

**Figure 3** below displays a clear current density decreasing in the case of Cinnamaldehyde extract existence in the corrosion system, indicating a good corrosion inhibition acting of the extract. Also the corrosion potential was almost constant and both cathodic and anodic Tafel slopes changed due to the presence of Cinnamaldehyde extract, showing a mixed behavior of Cinnamaldehyde molecules on A03081 surface, as the Cinnamaldehyde molecules could adsorb onto the cathodic and anodic sites, resulting in the mixed inhibition action.

From **Table 2** below, Cinnamaldehyde extract showed obvious lowering in the corrosion rate and the corresponding increase in the %IE for the Cinnamaldehyde extract. Due to the active sites on Cinnamaldehyde molecules represented in the heteroatoms and  $\pi$  bonds, they have the ability to adsorb and restrict the alloy surface's electrochemical processes [16, 17]. Finally, the shaped of PDP curves are almost the same in both uninhibited and inhibited 2.0 M HCl, showing the lack of effect of Cinnamaldehyde on the alloy corrosion mechanism.

The inhibition efficiency was measured using the equation [18, 19]:

$$\%IE_i = \left(1 - \frac{i_{Cin}}{i}\right) \times 100 \quad (3)$$

where,  $i_{Cin}$  and  $i$  are the current density of A03081 alloy in inhibited (using Cinnamaldehyde extract) and uninhibited 2.0 M HCl solution.

**Table 2:** Corrosion parameters of A03081 alloy in 2.0 M HCl solution with and without different Cinnamaldehyde concentrations at 298 K

Solution (ppm)	$\beta_a$ (mV/dec)	$-\beta_c$ (mV/dec)	$-E_{corr}$ (mV)	$i_{corr}$ (mA)	$CR_t$ (mm/year)	%IE <sub>i</sub>
Blank	119	98	730	4.6	50	-
10	123	100	771	2.5	27	45.65
40	125	115	728	1.9	21	58.70
80	131	113	766	1.2	13	73.91
120	133	121	737	0.7	8	84.78
120	133	122	737	0.3	3	93.48

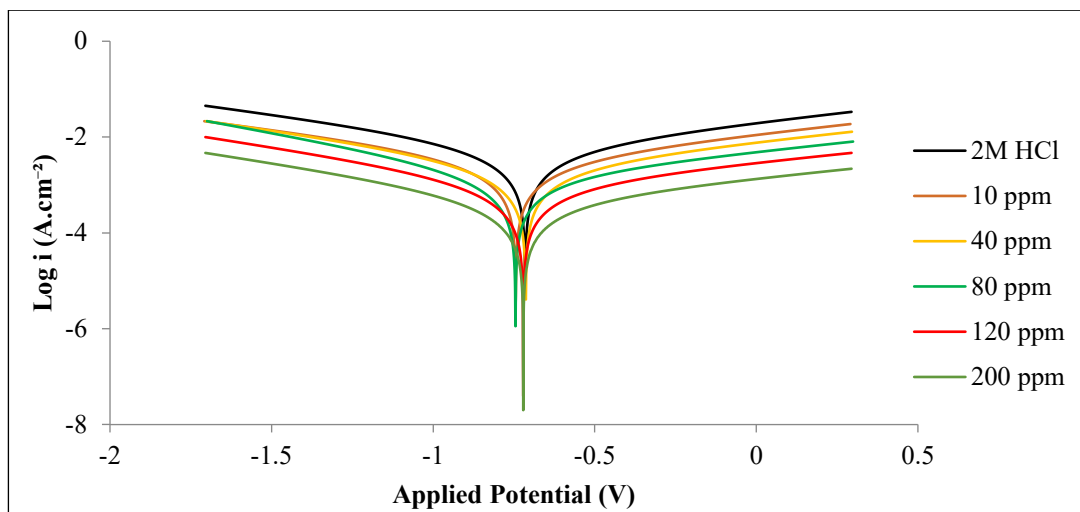


**Figure 3:** PDP curves of A03081 alloy in 2.0 M HCl solution with and without different Cinnamaldehyde extract concentrations at 298 K

### 3.2.2. Electrochemical Impedance Spectroscopy (EIS)

Fitting of the EIS data is done utilizing the equivalent circuit in **Figure 4**. **Figure 5** shows the corresponding Nyquist plots and Bode diagram. Inspecting the Nyquist plots clarifies a clear increasing of charge transfer resistance ( $R_{ct}$ ) of the corrosive medium as Cinnamaldehyde dose increases; an indication for the increasing %IE of Cinnamaldehyde extract with increasing its concentration [20]. However, the form of Nyquist plots did not change with Cinnamaldehyde presence indicating that Cinnamaldehyde doesn't change the corrosion mechanism, as shown above in PDP. Also, at low frequencies, the inductive loop appeared. The relaxation of both the oxide layer and the adsorbed species causes the capacitive behavior, which soon re-dissolve and induce the inductive loop [21].

The Bode diagram shows that the absolute charge transfer resistance  $|Z|$  of the system reached a peak at low frequencies due to the inductive action of the re-dissolved layers, however it increased with increasing Cinnamaldehyde concentration, confirming the inhibition efficiency. The figure also shows an overall increase in the phase shift of the constant phase element (the non-ideal capacitor) of the dielectric layer created on the alloy surface reaching ( $-67^\circ$ ) due to increasing in the Cinnamaldehyde concentration, indicating a smoother surface formed by cause of the Cinnamaldehyde molecules' adsorption on A03081 surface [22].

The inhibition efficiency and  $C_{dl}$  were measured using the equations [23, 24]:

$$\% IE_{R_{ct}} = \left(1 - \frac{R_{ct}}{R_{ct,Cin}}\right) \times 100 \quad (4)$$

$$C_{dl} = Y_0 W^{N-1} = Y_0 (2\pi f_{max})^{N-1} \quad (5)$$

where,  $R_{ct}$  and  $R_{ct,Cin}$  are the charge transfer resistance of corrosion reaction without and with Cinnamaldehyde extract.  $Y_0$  is the constant phase element in mS.s,  $f_{max}$  is the frequency at which the impedance's imaginary component is at its highest.

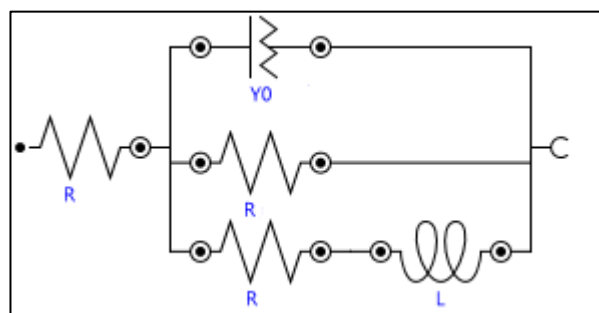


**Figure 4:** The suggested equivalent circuit for the EIS data of A03081 alloy in 2.0 M HCl

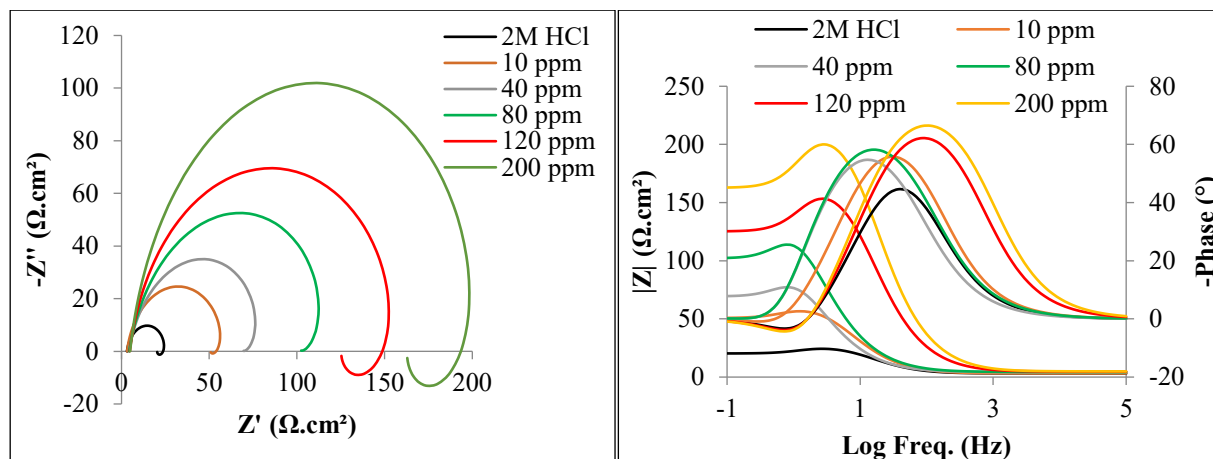


**Figure 5:** Nyquist plots (left) and Bode diagram (right) of A03081 alloy in 2.0 M HCl solution with and without different Cinnamaldehyde concentrations at 298 K

**Table 3:** EIS parameters of A03081 alloy in 2.0 M HCl solution with and without different Cinnamaldehyde concentrations at 298 K

Solution (ppm)	N	Y <sub>0</sub> (μF)	C <sub>dl</sub> (μF)	R <sub>s</sub> (Ω)	R <sub>ct</sub> (Ω)	R <sub>L</sub> (Ω)	L (H)	%IE <sub>Rct</sub>
Blank	0.75	5180	1785	3.1	48	18	54	-
10	0.77	3290	1564	3.2	308	51	670	84.27
40	0.79	2710	1376	4.2	500	80	700	90.31
80	0.80	1590	941	4.3	650	120	800	92.54
120	0.80	390	165	4.7	800	150	900	93.94
200	0.80	210	89	4.9	900	200	986	94.61

### 3.3. Adsorption isotherm

The A03081 alloy surface coverage ( $\theta$ ) was calculated with the help of weight loss readings. The relation between  $\theta$  and Cinnamaldehyde concentration is best fitted with Temkin adsorption isotherm, **Figure 6**, [25, 26]:

$$a\theta = \ln K_{ads} + \ln C_{cin} \quad (6)$$

where,  $K_{ads}$  and  $C_{cin}$  are the adsorption equilibrium constant and Cinnamaldehyde concentration, respectively.

The standard free energy of adsorption  $\Delta G^{\circ}_{ads}$  is calculated using the equation [27] and given in **Table 4**:

$$K_{ads} = \frac{1}{C_{H_2O}} \exp\left(\frac{-\Delta G^{\circ}_{ads}}{RT}\right) \quad (7)$$

where, R is the universal gas constant,  $C_{H_2O}$  is the concentration of water  $\approx 10^6$  ppm.

Also,  $\Delta G^{\circ}_{ads}$  values are in the range of (-33 to -35 kJ.mol<sup>-1</sup>) through 24 hours. The free electron pairs on O atom and the  $\pi$  bonds may cause electron transfer from some Cinnamaldehyde molecules to empty p-orbitals on the alloy surface. However, the released energy is not much enough that the inhibition action of Cinnamaldehyde is majorly due to a spontaneous electrostatic attraction between both the oppositely charged alloy surface and the Cinnamaldehyde species (physical adsorption) [28].

**Table 4:** Equilibrium constant and Gibbs free energy of adsorption of Cinnamaldehyde extract on A03081 alloy surface in 2.0 M HCl solution

Time (h)	R <sup>2</sup>	K <sub>ads</sub>	$\Delta G_{ads}$ (kJ/mol)
1	0.99	0.728	- 33.45
3	0.97	1.044	- 34.34
6	0.99	1.349	- 34.98
10	1.00	1.450	- 35.16
15	1.00	1.523	- 35.28
24	0.99	1.616	- 35.43

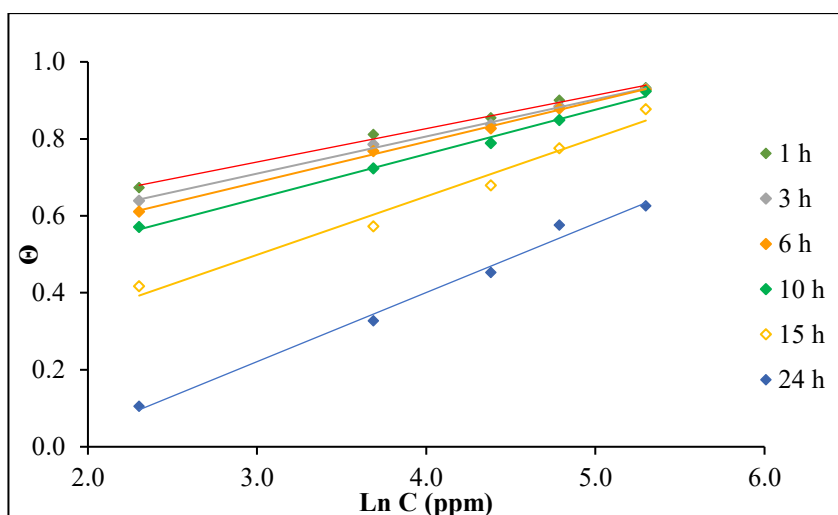


**Figure 6:** Temkin isotherm for the Cinnamaldehyde extract adsorption on A03081 alloy in 2.0 M HCl solution

### 3.4. Thermal effect and kinetic measurements

As shown in **Table 5**, the corrosion rate of A03081 alloy in both uninhibited and inhibited 2.0 M HCl solution increased with increasing temperature. However, Cinnamaldehyde extract showed a lower corrosion rate, hence a good inhibition action at elevated temperatures. The calculated inhibition efficiency of Cinnamaldehyde extract showed a noticeable decrease while temperature increases. This informs that the adsorption process was physical in action, as one can say that the adsorbed molecules of the extract are being desorbed with temperature elevating and this behavior can occur only in the case of physical adsorption process.

Applying Arrhenius equation [25]:

$$\ln CRt_{WL} = \left(\frac{-E_a}{RT}\right) + \ln A \quad (8)$$

and Transition-State theory [29]

$$\ln\left(\frac{CRt_{WL}}{T}\right) = \left(\ln\left(\frac{R}{N_A h}\right) + \left(\frac{\Delta S^*}{R}\right)\right) - \frac{\Delta H^*}{RT} \quad (9)$$

was the reference to measure the kinetic parameters of A03081 alloy in the present study.

As shown in **Table 5**, the activation energy ( $E_a$ ) required for the electrochemical reaction process has risen with only 200 ppm addition of Cinnamaldehyde extract. This suggests its contributing role in the inhibition process, by physically adsorbing onto the alloy surface, generating a veil between A03081 surface and the interacting acid [30]. Also, the increase in the enthalpy of activation value ( $\Delta H^*$ ); the energy absorbed from the surrounding environment is a good hint for a more energy required, is a clue for more difficult is the corrosion process. Finally, the more positive value of entropy of activation ( $\Delta S^*$ ) is an indication for randomness level the system has to be in for reaching the stable phase of adsorption process [31]. The change in the thermodynamic parameters shown indicate the aptitude of the Cinnamaldehyde molecules to stuck onto the alloy surface at elevated temperatures by the help of the of their functional groups. The Cinnamaldehyde structure shows aromatic ring,  $\pi$  electrons and oxygen atoms, all which act as electrostatic attractor for the charged metallic surface [32].

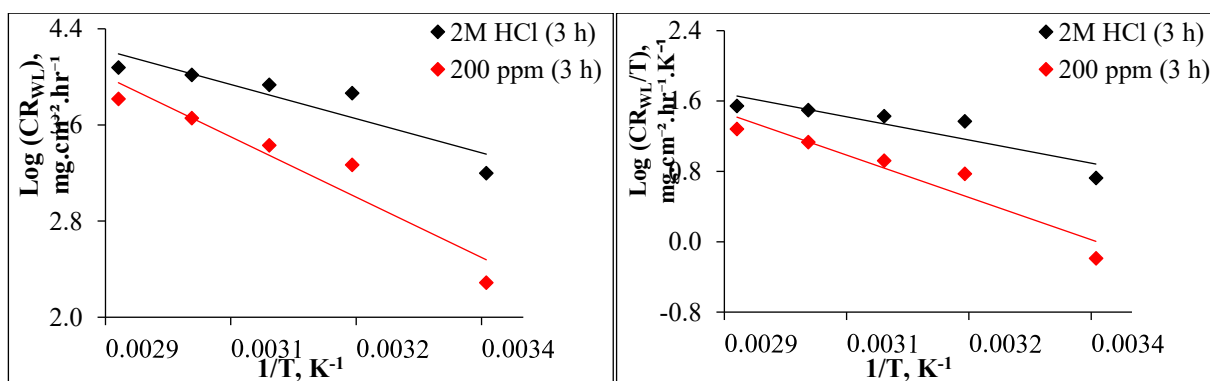


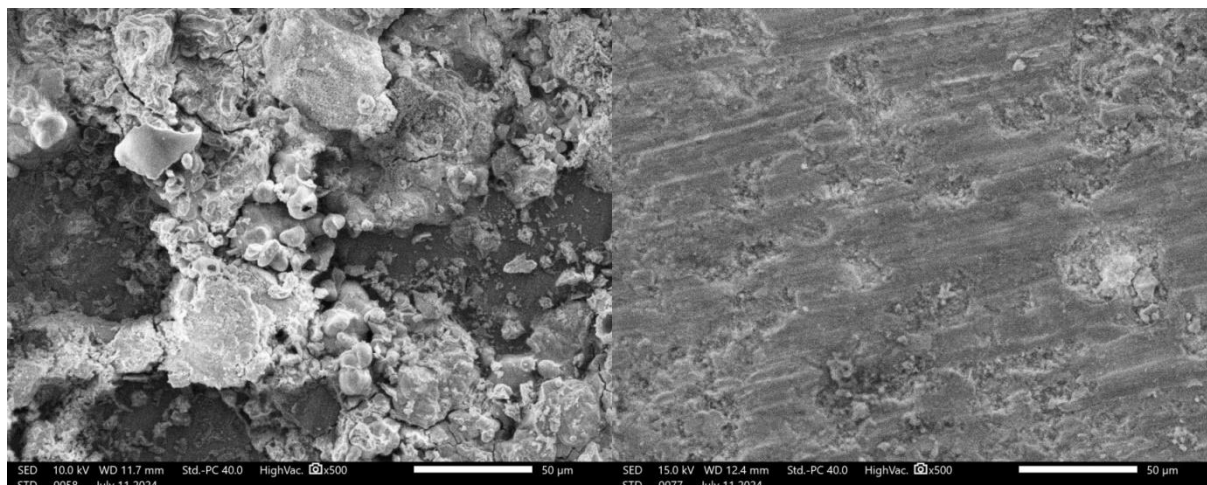
**Figure 7:** Arrhenius (left) and transition-state (right) plots

**Table 5:** Corrosion rate ( $CR_{TWL}$ ) in  $mg.h^{-1}.cm^{-2}$  and thermodynamic parameters of A03081 alloy in 2.0 M HCl solution with and without 200 ppm Cinnamaldehyde extract at different temperatures and 3 h immersion time

Solution	Temp. (°C)	$CR_{TWL}$	%IE <sub>WL</sub>	$\Delta E_a$ (kJ.mol <sup>-1</sup> )	$\Delta H^*$ (kJ.mol <sup>-1</sup> )	$\Delta S^*$ (J.mol <sup>-1</sup> .K <sup>-1</sup> )
Blank	25	1.57	-	36.29	33.64	-117.79
	40	7.30				
	50	8.58				
	60	10.37				
	70	11.92				
200 ppm	25	0.19	87.73	64.08	61.43	-101.63
	40	1.85	74.62			
	50	2.69	68.65			
	60	4.51	56.50			
	70	6.52	45.28			

### 3.5. SEM Analysis

In **Figure 8** below, the left SEM image shows the morphology of A03081 alloy coupon in 2.0 M HCl solution for three hours without Cinnamaldehyde extract and that the coupon is highly damaged. However, the right SEM image shows the A03081 surface becomes smoother with 200 ppm Cinnamaldehyde extract. These results prove that the Cinnamaldehyde extract adsorbed on the A03081 surface and generated a defense coating on the alloy surface, which protected the alloy surface from the corrosive acid medium [33].

**Figure 8:** SEM image for A03081 alloy in 2.0 M HCl solution (left) and SEM image for A03081 alloy in 2.0 M HCl solution in the presence of 200 ppm Cinnamaldehyde extract (right)

### 3.6. Quantum expectation and Monte Carlo simulations

After getting the optimized structure for Cinnamaldehyde molecule, Gaussian 09 gave us the quantum parameters from which we could understand the reactivity and the adsorption mechanism of the tested structure. The quantum parameters;  $E_{HOMO}$ , the highest occupied molecular orbital energy,  $E_{LUMO}$ , the lowest occupied molecular orbital energy, the ionization potential ( $I = -E_{HOMO}$ ), the electron affinity ( $A = -E_{LUMO}$ ), the electronegativity ( $\chi$ ), the absolute hardness ( $\eta$ ), and the number of transferred electrons ( $\Delta N$ ) are shown in **Table 6** with the help of the following equations [34, 35]:

$$\Delta N = \frac{\chi_{Al} - \chi_{Cin}}{2(\eta_{Al} + \eta_{Cin})} \quad (10)$$

$$\chi = \frac{(I+A)}{2} \quad (11)$$

$$\eta = \frac{(I-A)}{2} \quad (12)$$

$$E_{int} = E_{tot} - (E_{Cin} + E_{Al+Solution}) \quad (13)$$

$$E_{ads} = -E_{int} \quad (14)$$

where  $\chi_{Al} = 3.23 \text{ eV.mol}^{-1}$ , the absolute electronegativity for Al [36],  $\chi_{Cin}$  the absolute electronegativity of Cinnamaldehyde,  $\eta_{Al} = 0$ , the absolute hardness of Al and  $\eta_{Cin}$  the absolute hardness of Cinnamaldehyde.

$E_{\text{HOMO}}$  and  $E_{\text{LUMO}}$  give information about donating and accepting electrons, respectively. An indicator for reactivity of the inhibitor compounds is the energy difference ( $\Delta E$ ) between HOMO and LUMO. More reactivity of a molecule is indicated by a smaller  $\Delta E$  value. It was also reported that if  $3.6 > \Delta N > 0$ , then the tested inhibitor can donate electrons to Al surface [37].

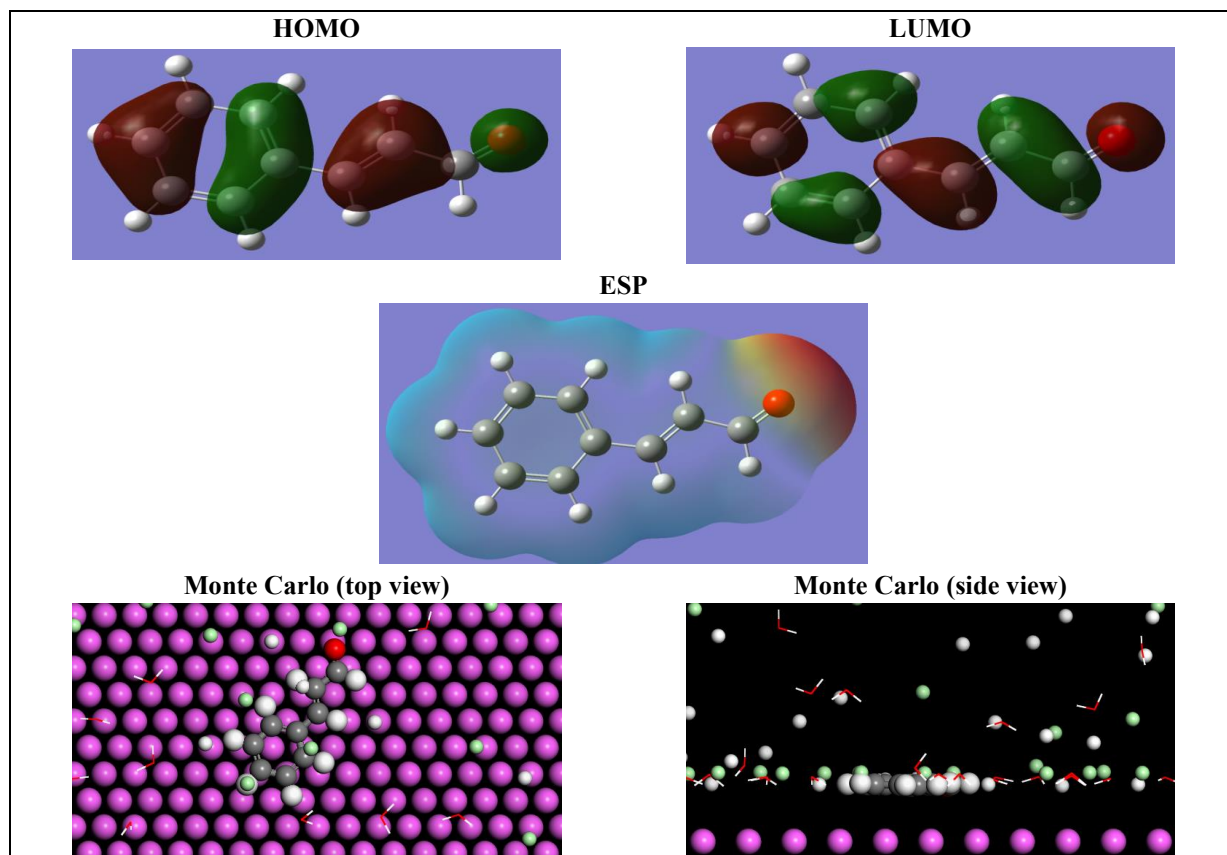


**Figure 9:** HOMO, LUMO, ESP of Cinnamaldehyde molecule and its adsorption simulation on Al (001)

The HOMO and LUMO orbitals were found around the whole molecule. A resonance is expected, **Figure 9**. Based on that, the performed Monte Carlo simulation showed a parallel adsorption of Cinnamaldehyde molecule on Al (001) surface, with a negative  $E_{\text{ads}}$  value (-447.81 kcal/mol); an indication for the spontaneous adsorption process [38].

Both the negative  $E_{\text{HOMO}}$  and the low  $\Delta N$  value refer to the more tendency of Cinnamaldehyde molecules to accept electrons rather than donate them. ESP showed both blue and red regions in the electrostatic potential mapping (blue in the most), which is indication for a poor electron density, in general, although the capability to donate electrons. And this is more likely to be physisorption rather than chemisorption as experimental results showed [39].

**Table 6:** Calculated parameters of Cinnamaldehyde structure optimization and simulation of Cinnamaldehyde molecule adsorption on Al (001)

Parameters	Value
$E_{\text{HOMO}}$ (eV)	-6.96
$E_{\text{LUMO}}$ (eV)	-2.52
$\Delta E$ (eV)	4.44
$I$ (eV)	6.96
$A$ (eV)	2.52
$\chi$ (eV)	4.74
$\eta$ (eV)	2.22
$\Delta N$	0.34
Total energy $E_{\text{tot}}$ (kcal/mol)	-347.54
Interaction energy $E_{\text{int}}$ (kcal/mol)	447.81
Adsorption energy $E_{\text{ads}}$ (kcal/mol)	-447.81

In conclusion, the tested Cinnamaldehyde extract interacts with the aluminum surface through physisorption in most, wherein the pre-adsorbed ( $\text{Cl}^-$ ) ions and/or the (Al-O) negative sites electrostatically attract Cinnamaldehyde molecules to the Al surface. Also, some Cinnamaldehyde molecules could donate electrons to the empty p-orbitals of Al surface, covering the aluminum surface from acid exposure [40].

#### 4. Conclusion

- Cinnamaldehyde can be extracted from Cinnamon using chloroform.
- Cinnamaldehyde showed inhibition efficiency exceeded 90% for A03081 alloy in acid solution.
- Weight loss and electrochemical measurements revealed that the %IE of Cinnamaldehyde increases with increasing concentration and decreasing temperature.
- The adsorption of Cinnamaldehyde molecules on A03081 alloy followed Temkin isotherm.
- The adsorption process was found to be predominantly physical and spontaneous.

#### 5. References

- [1] R. Comizzoli, R. Frankenthal, P. Milner, J. Sinclair, Corrosion of electronic materials and devices, *Science*, 234 (1986) 340-345.
- [2] D. Dwivedi, K. Lepková, T. Becker, Carbon steel corrosion: a review of key surface properties and characterization methods, *RSC advances*, 7 (2017) 4580-4610.
- [3] A. Al-Turkustani, S. Arab, R. Al-Dahiri, Aloe plant extract as environmentally friendly inhibitor on the corrosion of aluminum in hydrochloric acid in absence and presence of iodide ions, *Modern Applied Science*, 4 (2010) 105.
- [4] A. Singh, Y. Lin, W. Liu, S. Yu, J. Pan, C. Ren, D. Kuanhai, Plant derived cationic dye as an effective corrosion inhibitor for 7075 aluminum alloy in 3.5% NaCl solution, *Journal of Industrial and Engineering Chemistry*, 20 (2014) 4276-4285.
- [5] M. Prabakaran, S.-H. Kim, A. Sasireka, K. Kalaiselvi, I.-M. Chung, Polygonatum odoratum extract as an eco-friendly inhibitor for aluminum corrosion in acidic medium, *Journal of adhesion science and Technology*, 32 (2018) 2054-2069.
- [6] E.E. El-Katori, S. Al-Mhyawi, Assessment of the *Bassia muricata* extract as a green corrosion inhibitor for aluminum in acidic solution, *Green chemistry letters and Reviews*, 12 (2019) 31-48.
- [7] T.H. Pham, W.-H. Lee, J.-G. Kim, Chrysanthemum coronarium leaves extract as an eco-friendly corrosion inhibitor for aluminum anode in aluminum-air battery, *Journal of Molecular Liquids*, 347 (2022) 118269.
- [8] P. Kwolek, K. Dychtoń, B. Kościelniak, A. Obłój, A. Podborska, M. Wojnicki, Gallic acid as a potential green corrosion inhibitor for aluminum in acidic solution, *Metals*, 12 (2022) 250.
- [9] M. Chowdhury, M. Ahmed, N. Hossain, M. Islam, S. Islam, M. Rana, Tulsi and green tea extracts as efficient green corrosion inhibitor for the corrosion of aluminum alloy in acidic medium, *Results Eng.* 17 (2023), 100996, in, 2023.
- [10] C.M. Méndez, C.A. Gervasi, G. Pozzi, A.E. Ares, Corrosion inhibition of aluminum in acidic solution by *Ilex paraguariensis* (Yerba Mate) extract as a green inhibitor, *Coatings*, 13 (2023) 434.
- [11] H.A. Abdullah, R.A. Anaee, A.A. Khadom, A.T. Abd Ali, A.H. Malik, M.M. Kadhim, Experimental and theoretical assessments of the chamomile flower extract as a green corrosion inhibitor for aluminum in artificial seawater, *Results in Chemistry*, 6 (2023) 101035.
- [12] N. Hossain, M.A. Chowdhury, M. Rana, M. Hassan, S. Islam, Terminalia arjuna leaves extract as green corrosion inhibitor for mild steel in HCl solution, *Results in Engineering*, 14 (2022) 100438.
- [13] H. Hussien, S. Shahen, A.M. Abdel-karim, I.M. Ghayad, O.A. El-Shamy, N. Mostfa, N.E.-d. Ahmed, Experimental and theoretical evaluations: Green synthesis of new organic compound bis ethanethiopyl oxalamide as corrosion inhibitor for copper in 3.5% NaCl, *Egyptian Journal of Chemistry*, 66 (2023) 189-196.
- [14] A. El-Etre, A.H. Tantawy, S. Eid, D.F. Seyam, Research article open access corrosion inhibition of aluminum by novel amido-amine based cationic surfactant in 0.5 M HCl solution, *Journal of Basic and Environmental Sciences*, 2 (2017) 128-139.
- [15] Z. Zheng, J. Hu, N. Eliaz, L. Zhou, X. Yuan, X. Zhong, Mercaptopropionic acid-modified oleic imidazoline as a highly efficient corrosion inhibitor for carbon steel in  $\text{CO}_2$ -saturated formation water, *Corrosion Science*, 194 (2022) 109930.
- [16] D.F. Seyam, S. Eid, A.H. Tantawy, Study the Inhibition effect of Three Newly Synthesized Schiff Base Based Cationic Surfactants on Aluminum Corrosion in 0.5 M HCl Solution, *Egyptian Journal of Chemistry*, 66 (2023) 87-99.
- [17] M. Abou Elsaoud, A. El-Kattan, A. El-Etre, Test of No Plac Expired Drug as Metallic Corrosion Inhibitor for Carbon Steel, *Benha Journal of Applied Sciences*, 6 (2021) 239-245.
- [18] S. Ren, M. Cui, X. Chen, S. Mei, Y. Qiang, Comparative study on corrosion inhibition of N doped and N, S codoped carbon dots for carbon steel in strong acidic solution, *Journal of Colloid and Interface Science*, 628 (2022) 384-397.
- [19] E. Fouad, M. Abd El-Moneim, M.M. ElDesouky, W.I. Eldougoud, The Synthesis of New Corrosion Inhibitors Based on Modified Chitosan to Provide Protection over Mild Steel, *Egyptian Journal of Chemistry*, 66 (2023) 283-289.
- [20] M. Alfakeer, R.N. Felaly, S.S. Al-Juaid, D. Seyam, E. Mabrouk, M. Abdallah, Synthesis and cyclic voltammetric studies of azo dye compounds derived from 1, 5-dihydroxynaphthalene and their application as corrosion inhibitors for carbon steel in hydrochloric acid solution, *International Journal of Electrochemical Science*, 20 (2025) 100892.
- [21] J. Haque, M. Zulaikha, W.W. Nik, W. Daoudi, E. Berdimurodov, F. Zulkifli, Alocasia Odora Extract as Environmentally Benign Corrosion Inhibitor for Aluminum in HCl, *Moroccan Journal of Chemistry*, 11 (2023) 11-14 (2023) 1013-1026.

- [22] D.F. Seyam, A. H. Tantawy, S. Eid, A.Y. El-Etre, Study of the inhibition effect of two novel synthesized amido-amine-based cationic surfactants on aluminum corrosion in 0.5 M HCl solution, *Journal of Surfactants and Detergents*, 25 (2022) 133-143.
- [23] M. Rezaeivala, S. Karimi, K. Sayin, B. Tüzün, Experimental and theoretical investigation of corrosion inhibition effect of two piperazine-based ligands on carbon steel in acidic media, *Colloids and surfaces a: physicochemical and engineering aspects*, 641 (2022) 128538.
- [24] A.M. Ashmawy, M. Mostfa, Study of eco-friendly corrosion inhibition for mild steel in acidic environment, *Egyptian Journal of Chemistry*, 64 (2021) 1285-1291.
- [25] S. Wan, H. Wei, R. Quan, Z. Luo, H. Wang, B. Liao, X. Guo, Soybean extract firstly used as a green corrosion inhibitor with high efficacy and yield for carbon steel in acidic medium, *Industrial Crops and Products*, 187 (2022) 115354.
- [26] C.G. Vaszilcsin, M.V. Putz, A. Kellenberger, M.L. Dan, On the evaluation of metal-corrosion inhibitor interactions by adsorption isotherms, *Journal of Molecular Structure*, 1286 (2023) 135643.
- [27] A.S. Jasim, K.H. Rashid, K.F. AL-Azawi, A.A. Khadom, Synthesis of a novel pyrazole heterocyclic derivative as corrosion inhibitor for low-carbon steel in 1M HCl: Characterization, gravimetric, electrochemical, mathematical, and quantum chemical investigations, *Results in Engineering*, 15 (2022) 100573.
- [28] A.H. Tantawy, K.A. Soliman, H.M. Abd El-Lateef, Novel synthesized cationic surfactants based on natural piper nigrum as sustainable-green inhibitors for steel pipeline corrosion in CO<sub>2</sub>-3.5% NaCl: DFT, Monte Carlo simulations and experimental approaches, *Journal of Cleaner Production*, 250 (2020) 119510.
- [29] B. Tan, B. Xiang, S. Zhang, Y. Qiang, L. Xu, S. Chen, J. He, Papaya leaves extract as a novel eco-friendly corrosion inhibitor for Cu in H<sub>2</sub>SO<sub>4</sub> medium, *Journal of colloid and interface science*, 582 (2021) 918-931.
- [30] M.A. Abbas, A.S. Ismail, K. Zakaria, A. El-Shamy, S.Z. El Abedin, Adsorption, thermodynamic, and quantum chemical investigations of an ionic liquid that inhibits corrosion of carbon steel in chloride solutions, *Scientific Reports*, 12 (2022) 12536.
- [31] O.P. Nsude, K.J. Orie, Thermodynamic and adsorption Analysis of corrosion inhibition of mild steel in 0.5 M HCl medium via ethanol extracts of *Phyllanthus mellerianus*, *American Journal of Applied Chemistry*, 10 (2022) 67-75.
- [32] A.A. Elsaoud, E.M. Mabrouk, D.F. Seyam, A. El-Etre, Recyclization of expired Megavit Zinc (MZ) drug as metallic corrosion inhibitor for copper alloy C10100 in nitric acid solution, *Journal of Bio-and Tribo-Corrosion*, 7 (2021) 1-9.
- [33] R. Felaly, M. Alfakeer, A.A. Ali, S.S. Al-Juaid, E.M. Mabrouk, A. El-Etre, D.F. Seyam, M. Abdallah, Enhanced corrosion protection of copper alloy in 2.0 M HNO<sub>3</sub> solution using expired solo sept, slim-lax and well derm drugs, *International Journal of Electrochemical Science*, (2024) 100657.
- [34] X. Xu, H. Xu, W. Li, Y. Wang, X. Zhang, A combined quantum chemical, molecular dynamics and Monte Carlo study of three amino acids as corrosion inhibitors for aluminum in NaCl solution, *Journal of Molecular Liquids*, 345 (2022) 117010.
- [35] M. Abdallah, M. Alfakeer, R.N. Felaly, A.M. Almohyawi, J.H. Al-Fahemi, S.S. Al-Juaid, D.F. Seyam, E.M. Mabrouk, K.A. Soliman, Evaluation of porphyrin molecules as effective corrosion inhibitors for copper alloy in sulfuric acid using both experimental and computational approaches: Original scientific paper, *Journal of Electrochemical Science and Engineering*, (2025) 2544-2544.
- [36] M. Abdallah, E. Gad, M. Sobhi, J.H. Al-Fahemi, M. Alfakeer, Performance of tramadol drug as a safe inhibitor for aluminum corrosion in 1.0 M HCl solution and understanding mechanism of inhibition using DFT, *Egyptian Journal of Petroleum*, 28 (2019) 173-181.
- [37] S. Bashir, A. Thakur, H. Lgaz, I.-M. Chung, A. Kumar, Corrosion inhibition efficiency of bronopol on aluminium in 0.5 M HCl solution: Insights from experimental and quantum chemical studies, *Surfaces and Interfaces*, 20 (2020) 100542.
- [38] A.S. Al-Gorair, R. Felaly, N. Fouad, S.S. Al-Juaid, D.F. Seyam, N. Saadan, A.Y. El-Etre, E.M. Mabrouk, M. Abdallah, Corrosion kinetics of carbon steel in hydrochloric acid and its inhibition by recycling Salbutamol extracted from expired Farcolin drug, *Green Chemistry Letters and Reviews*, 17 (2024) 2413418.
- [39] M. Abdallah, A.S. Al-Gorair, H. Hawsawi, F. Al-abdali, D.F. Seyam, S.S. Al-Juaid, E. Elmoosalamy, R.S.A. Hameed, K. Soliman, M. Motawea, Assessment of quinazoline derivatives as efficient corrosion inhibitor for carbon steel in acidic environment. A theoretical and practical analysis, *International Journal of Electrochemical Science*, 20 (2025) 100990.
- [40] N.O. Eddy, S.A. Odoemelam, E.C. Ogoko, R.A. Ukpe, R. Garg, B. Anand, Experimental and quantum chemical studies of synergistic enhancement of the corrosion inhibition efficiency of ethanol extract of *Carica papaya* peel for aluminum in solution of HCl, *Results in Chemistry*, 4 (2022) 100290.